

***In vitro* effects of chitosan nanoparticles on proliferation of human gastric carcinoma cell line MGC803 cells**

Li-Feng Qi, Zi-Rong Xu, Yan Li, Xia Jiang, Xin-Yan Han

Li-Feng Qi, Zi-Rong Xu, Yan Li, Xia Jiang, Xin-Yan Han, Nano-biology Laboratory of Animal Science College, Zhejiang University, Hangzhou 310029, Zhejiang Province, China

Co-first-authors: Li-Feng Qi and Zi-Rong Xu

Correspondence to: Dr. Li-Feng Qi, Nano-biology Laboratory of Animal Science College, Zhejiang University, Hangzhou 310029, Zhejiang Province, China. lifengqi01@hotmail.com

Telephone: +86-571-86971075 Fax: +86-571-86994963

Received: 2004-12-06 Accepted: 2005-01-26

Abstract

AIM: To investigate the effects of chitosan nanoparticles on proliferation of human gastric carcinoma cell line MGC803 *in vitro* and the possible mechanisms involved.

METHODS: Chitosan nanoparticles were characterized by particle size, zeta potential, and morphology. After treatment with various concentrations of chitosan nanoparticles (25, 50, 75, 100 µg/mL) at various time intervals, cell proliferation, ultrastructural changes, DNA fragmentation, mitochondrial membrane potential (MMP), cell cycle phase distribution and apoptotic peaks of MGC803 cells were analyzed by MTT assay, electron microscopy, DNA agarose gel electrophoresis, and flow cytometry.

RESULTS: Chitosan nanoparticles exhibited a small particle size as 65 nm and a high surface charge as 52 mV. Chitosan nanoparticles markedly inhibited cell proliferation of MGC803 cells with an IC₅₀ value of 5.3 µg/mL 48 h after treatment. After treatment with chitosan nanoparticles, the typical necrotic cell morphology was observed by electron microscopy, a typical DNA degradation associated with necrosis was determined by DNA agarose electrophoresis. Flow cytometry showed the loss of MMP and occurrence of apoptosis in chitosan nanoparticles-treated cells.

CONCLUSION: Chitosan nanoparticles effectively inhibit the proliferation of human gastric carcinoma cell line MGC803 *in vitro* through multiple mechanisms, and may be a beneficial agent against human carcinoma.

© 2005 The WJG Press and Elsevier Inc. All rights reserved.

Key words: Chitosan nanoparticles; Gastric carcinoma; Necrosis; Apoptosis

Qi LF, Xu ZR, Li Y, Jiang X, Han XY. *In vitro* effects of chitosan nanoparticles on proliferation of human gastric carcinoma cell line MGC803 cells. *World J Gastroenterol* 2005; 11(33): 5136-5141

<http://www.wjgnet.com/1007-9327/11/5136.asp>

INTRODUCTION

Chitosan, the deacetylated derivative of chitin, is one of the abundant, renewable, nontoxic and biodegradable carbohydrate polymers, and available largely in the exoskeletons of shellfish and insects. Chitosan has been widely applied as a functional biopolymer in food and pharmaceuticals. Chitosan is known to have various biological activities including immunoenhancing effects, antitumoral, antifungal, and antimicrobial activities^[1-3]. Chitosan nanoparticles have been previously synthesized as drug carriers^[4-6]. In our previous reports, chitosan nanoparticles are prepared and characterized to investigate their heavy metal sorption, antibacterial, and antitumor activities^[7-9]. The unique characteristics of chitosan nanoparticles could provide a higher affinity for negatively charged biological membranes and site-specific targeting *in vivo*^[7]. Chitosan nanoparticles could elicit dose-dependent inhibitory effects on the proliferation of various tumor cell lines, while low toxicity against normal human liver cells^[9].

In this paper, *in vitro* effects of chitosan nanoparticles on the proliferation of human gastric carcinoma (MGC803) cells were studied to illustrate the possible mechanisms involved. Cell viability was determined by MTT assay, necrotic cell morphology and DNA fragmentation were observed by electron microscopy and DNA agarose electrophoresis. Changes of mitochondrial membrane potential (MMP), cell cycle, and apoptotic peaks were analyzed by flow cytometry.

MATERIALS AND METHODS

Characterization of chitosan nanoparticles

Chitosan nanoparticles were prepared as described previously^[7,8]. Particle size distribution and zeta potential of chitosan nanoparticles were determined using Zetasizer Nano-ZS90 (Malvern Instruments). The analysis was performed at a scattering angle of 90° at 25 °C using samples diluted to different intensity concentrations with de-ionized distilled water. Transmission electron microscopy (TEM, JEM-1200EX) was used to determine the morphology of chitosan nanoparticles.

Cell line and cell culture

Human gastric carcinoma MGC803 cell line was obtained from the Cell Bank of the Chinese Academy of Sciences, Shanghai, China. The cell line was cultured in RPMI-1640 supplemented with 10% heat-inactivated fetal bovine serum (GIBCO). The cell cultures were maintained at 37 °C in a humidified incubator in an atmosphere of 95% air and 50 mL/L CO₂.

Cell viability assay

In the case of floating MGC803 cells, 100 µL aliquot of

cell suspension containing 10^6 cells was added to each well of a 96-well plate (Corning, USA). After being cultured for 24 h, the cells were immediately treated with various doses (25, 50, 75, 100 $\mu\text{g}/\text{mL}$) of chitosan nanoparticles for another 24 or 48 h. The effect of different treatments on cell viability was assessed by the tetrazolium dye assay^[10].

Scanning electron microscopy (SEM)

MGC803 cells grown on glass coverslips were incubated with 100 $\mu\text{g}/\text{mL}$ chitosan nanoparticles at intervals from 30 min to 4 h. The appropriate solvent was added to the control. Chitosan nanoparticles-treated and untreated cells were fixed in glutaraldehyde/paraformaldehyde solution and prepared for SEM by the triple-fixation GTGO methods. Briefly, the glutaraldehyde/paraformaldehyde-fixed cell monolayer was post-fixed by 2% osmium tetroxide (OsO_4) and the final fixation step was performed by 2% tannic acid/guanidine hydrochloride. Thereafter, the cells were dehydrated in graded ethanol solutions, ethanol was exchanged by graded solutions of Freon 113, and the cells were air-dried and gold-coated using a Polaron sputter coater. The surface morphology of cells was examined by a XL30-ESEM scanning electron microscope.

Transmission electron microscopy (TEM)

MGC803 cells grown on glass coverslips were incubated with 100 $\mu\text{g}/\text{mL}$ chitosan nanoparticles for 24 h. The appropriate solvent was added to the controls. Chitosan nanoparticles-treated and untreated cells were fixed in glutaraldehyde/paraformaldehyde solution and prepared for TEM as previously described^[11]. Observations and micrographs were made under a JEM-1200EX TEM.

DNA fragmentation

After treatment with 100 $\mu\text{g}/\text{mL}$ chitosan nanoparticles for 6 or 24 h, cells were collected, washed with PBS, and lysed with a solution containing 10 mmol/L Tris-HCl pH 7.4, 10 mmol/L EDTA and 0.5% Triton X-100. The lysates were incubated with 200 mg/mL RNase A (Sigma) for 1 h followed by 200 mg/mL proteinase K (GIBCO) for 1 h at 37 °C. These samples were then extracted with phenol/chloroform/isoamyl alcohol (25:24:1, v/v/v) followed by chloroform. DNA was precipitated in two volumes of ethanol in the presence of 0.3 mol/L sodium acetate. The DNA samples thus obtained were run on 1.5% agarose gel at 50 V and visualized by ethidium bromide staining under UV light.

Determination of mitochondrial membrane potential

To study the MMP, MGC803 cells were treated with various concentrations of chitosan nanoparticles (25, 50, 75, 100 $\mu\text{g}/\text{mL}$) for 4 h, and then stained with 10 $\mu\text{g}/\text{mL}$ rhodamine 123 (Sigma) for 30 min, which is easily sequestered by the mitochondrial membrane^[12]. Once the MMP was lost, rhodamine 123 was subsequently washed out of the cells. The MMP was determined using a FACSCalibur flow cytometer (Becton Dickinson, San Jose, CA) and analyzed by a CellQuest software program (BD PharMingen, Franklin Lakes, USA).

Cell cycle analysis

Flow cytometry was employed to determine the DNA

content and the apoptotic peaks of the cells. MGC803 cells were seeded on 100-mm dishes and grown in RPMI-1640 supplemented with 10% fetal bovine serum. After being treated with various concentrations of chitosan nanoparticles (25, 50, 75, 100 $\mu\text{g}/\text{mL}$) for 24 h, the cells were harvested, trypsinized, washed with PBS, fixed by adding slowly 2 mL of cold 70% ethanol into the tube and then stored at 4 °C. After fixation, the cells were washed, centrifuged, and resuspended in 0.05 mg/mL propidium iodide (Sigma, USA), 100 U/mL RNase (Sigma, USA) in PBS. The sample was incubated for 30 min at room temperature in the dark, and analyzed on a FACSCalibur flow cytometer. Cell cycle data originally obtained with CellQuest software were re-analyzed using ModFit software (Verity Software House, Topsham, USA). At the same time negative controls were constructed.

RESULTS

Size, zeta potential, and morphology of chitosan nanoparticles

The average particle size of chitosan nanoparticles was 65 nm and the size distribution ranged from 46 to 83 nm (Figure 1). Zeta potential, i.e., surface charge greatly influenced the particle stability in suspension through the electrostatic repulsion between the particles. It could also determine the interaction of nanoparticles *in vivo* with the tumor cell membrane, which was usually negatively charged. Chitosan nanoparticles had a positive charge about 52 mV (Figure 2A), much higher than that of chitosan in 0.25% acetic acid solution (Figure 2B). A solid dense structure and a round shape of chitosan nanoparticles were shown under TEM (Figure 3).

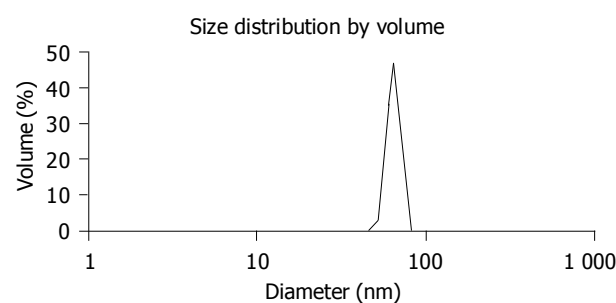


Figure 1 Size distribution of chitosan nanoparticles.

Cell viability assay

In this study, the exponentially grown gastric carcinoma MGC803 cells were treated with various concentrations of chitosan nanoparticles ranging from 25 to 100 $\mu\text{g}/\text{mL}$, and the cell viability was measured by the MTT assay. The inhibition of cell viability by chitosan nanoparticles was clearly observed in a dose- and time-dependent manner (Figure 4). The median lethal concentration of chitosan nanoparticles was 16.2 and 5.3 $\mu\text{g}/\text{mL}$ for MGC803 cells at 24 and 48 h, respectively.

Necrotic cell morphology

Necrosis is known to occur due to the disruption of cellular and nuclear membranes under extreme physiological stimuli.

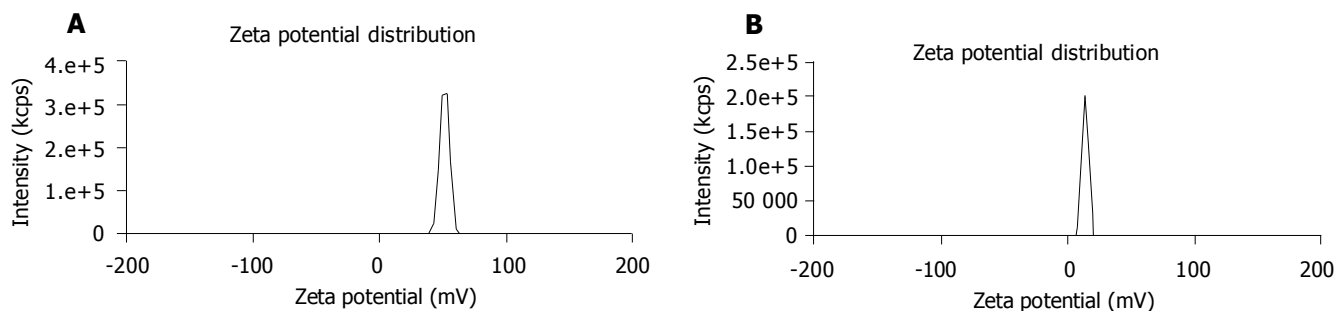


Figure 2 Zeta potential distribution of chitosan nanoparticles (A) and chitosan (B) in 0.25% acetic acid solution.

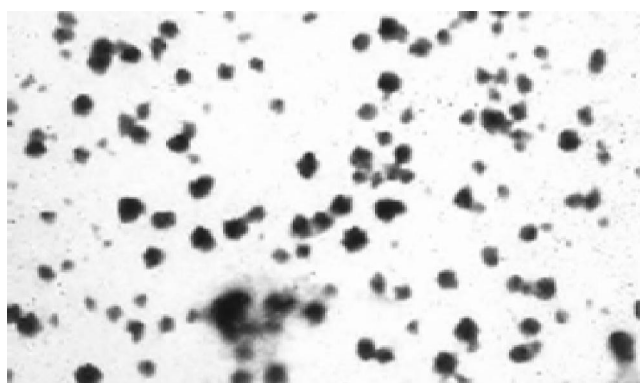


Figure 3 TEM photograph of chitosan nanoparticles. The bar stands for 100 nm.

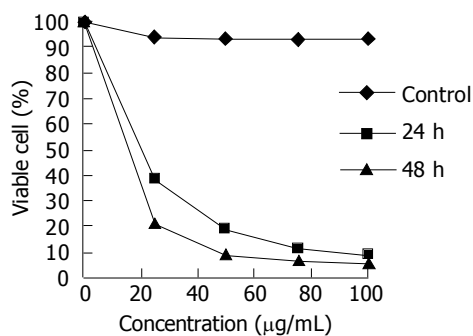


Figure 4 Inhibition of chitosan nanoparticles on MGC803 cell proliferation.

Rupture of the cellular membrane is one of the crucial criteria used to distinguish necrosis from apoptosis^[12]. The ultrastructural alterations of MGC803 cells treated with chitosan nanoparticles were observed under scanning electron microscope and transmission electron microscope. MGC803 cells treated with chitosan nanoparticles displayed typical morphological features of necrosis. Control MGC803 cells showed their normal shape and surface morphology under SEM (Figure 5). The cell surface showed the presence of numerous, randomly distributed microvilli. Cell death induced by chitosan nanoparticles showed the features of necrosis as evidenced by an early membrane leakage and the microvilli reduction after 30-min treatment. Microvilli disappeared and irregular tiny holes appeared on the cells' surface when treated for 2 h, with fracturing membrane

solubilization. MGC803 cells appeared extensively damaged. The cells that broke into pieces were observed as honeycomb shape after 4-h treatment. The loss of membrane integrity and pore forming surface morphology suggested a necrotic type of cell death and the unique mechanism of interaction between chitosan nanoparticles and plasma membrane.

Necrotic morphological features of MGC803 cells treated with chitosan nanoparticles such as disruption of the cytoplasm and appearance of remnants of swollen organelles were also revealed under TEM (Figure 6). Untreated cells showed integral membrane distributed with microvilli and normal organelle. While treated with chitosan nanoparticles for 24 h, cells became vacuolated, the plasma membrane was disrupted completely, and the content in the cells leaked out.

DNA fragmentation

DNA was extracted from cultured MGC803 cells treated with 100 µg/mL chitosan nanoparticles for 6 or 24 h, the occurrence of necrosis was detected by agarose gel electrophoresis. Specific DNA degradative smearing typical of necrotic degeneration^[13] was prominent in cells incubated with chitosan nanoparticles for 6 h, and the fragmented DNA increased greatly in cells treated for 24 h (Figure 7).

Alterations of mitochondrial membrane potential (MMP)

One possible mechanism involved in the necrosis of MGC803 cells induced by chitosan nanoparticles is mitochondrial damage. In this study, chitosan nanoparticles caused a dose-dependent decrease of MMP in MGC803 cells treated for 4 h (Figure 8). The percentage of cells with the loss of MMP increased significantly with the increase of chitosan nanoparticles concentration, and reached 74% when treated with 100 µg/mL chitosan nanoparticles. The strong dissipation in MMP suggested a possible disruption of cell mitochondrial membrane after chitosan nanoparticle treatment.

Cell cycle effects

The effects of chitosan nanoparticles on cell cycle progression, population distribution and apoptotic incidence in MGC803 cells were determined by flow cytometry. Chitosan nanoparticles-induced effects were detected by comparing the cell cycle profiles between nanoparticles-treated and untreated cells. Results demonstrated a significant decrease of cells in the G₀/G₁ phase (Table 1). Apoptotic peaks were observed

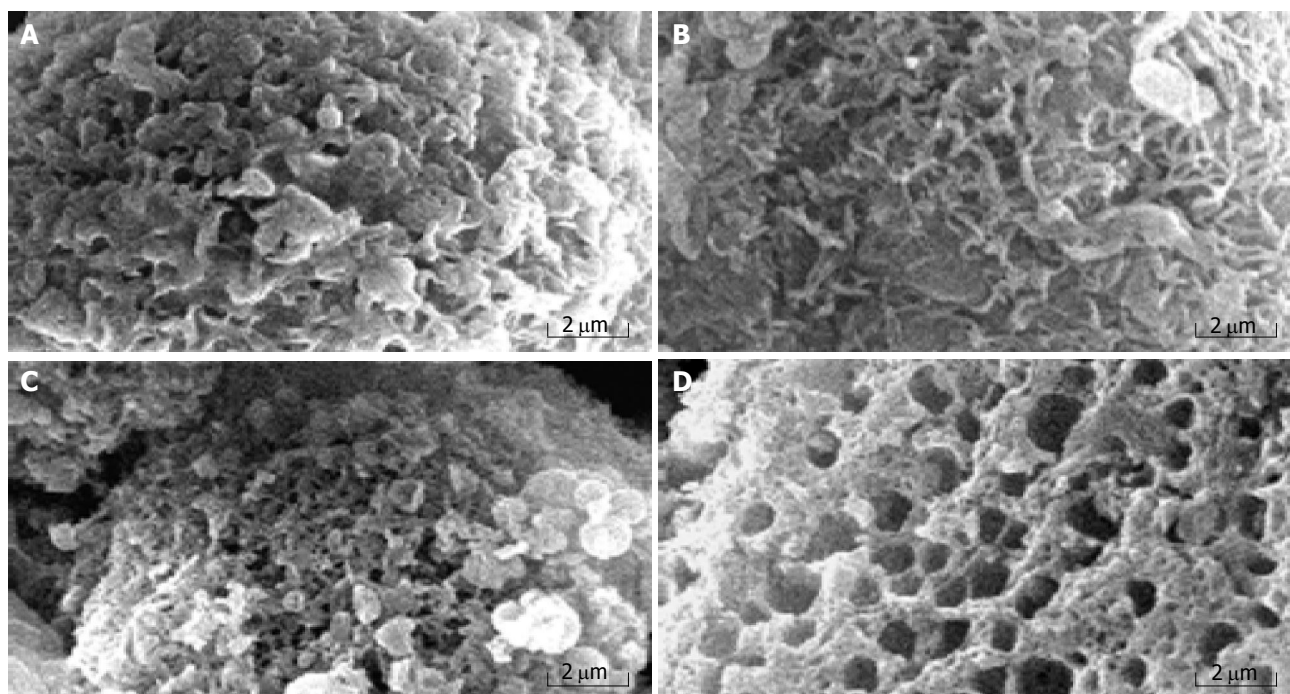


Figure 5 Surface morphology of control cells (A) and MGC803 cells treated with 100 µg/mL chitosan nanoparticles for 30 min (B), 2 h (C), and 4 h (D).

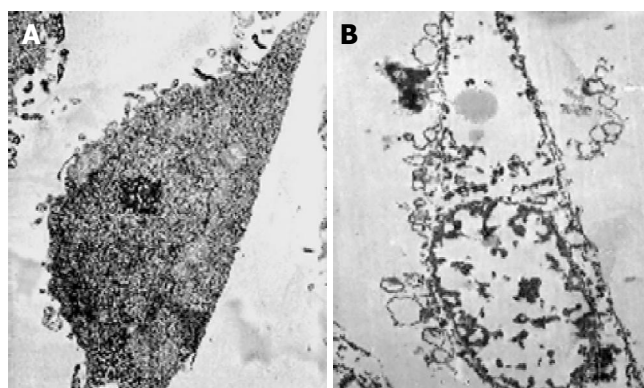


Figure 6 Transmission electron microscopic photographs of MGC803 cells cultured for 24 h in the absence (A) or presence of 100 µg/mL chitosan nanoparticles (B) *in vitro* (TEM, ×5 000).

and cell apoptotic incidence increased in a dose-dependent manner after chitosan nanoparticle treatment. The apoptotic incidence increased to 9.9% after being treated with 100 µg/mL chitosan nanoparticles (Figure 9).

DISCUSSION

Due to its reported biocompatibility and biodegradability^[14], chitosan has been applied in drug delivery systems to prepare microspheres or nanospheres for encapsulation of drugs, enzymes, proteins, and DNA^[15-17]. Chitosans could be developed as sole drugs for its biological activities. Soluble chitosan and chitosan microspheres are reported to show some degree of toxicity towards a murine melanoma cell line, B16F10, chitosan hydrochloride is most toxic having an IC_{50} of 0.21 ± 0.04 mg/mL^[18]. Amino-derivatized cationic chitosan derivatives show dose-dependent inhibitory effects on the

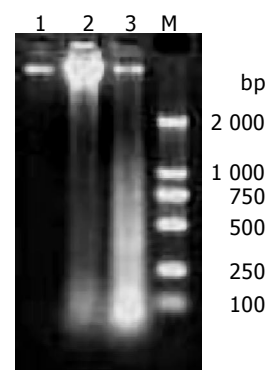


Figure 7 Agarose gel electrophoretic analysis of DNA isolated from MGC803 cells incubated with 100 µg/mL chitosan nanoparticles for 6 h (lane 2) and 24 h (lane 3) or without treatment (lane 1). M: a DNA marker.

proliferation of several tumor cell lines, with a lowest IC_{50} of 22 ± 4 µg/mL towards liver cancer^[19].

Positively charged chitosan nanoparticles prepared by our laboratory exhibit a higher cytotoxicity than other chitosan derivatives against various tumor cell lines, and a low toxicity against normal human liver cells^[9]. The present study demonstrated that chitosan nanoparticles could exert a high cytotoxicity against human gastric carcinoma MGC803 cell line. The gastric carcinoma cell line has been proved to be sensitive to chitosan nanoparticles with an IC_{50} value of 5.3 µg/mL after 48-h treatment, suggesting that chitosan nanoparticles may be a good candidate for antitumoral drugs. Particle size of nanoparticles plays a crucial role in their antitumor activity and *in vivo* distribution^[20,21]. Smaller nanoparticles show a higher accumulation at tumor sites and prolong *in vivo* half-life due to their avoidable capture by the reticuloendothelial system^[22,23]. Here, the particle size

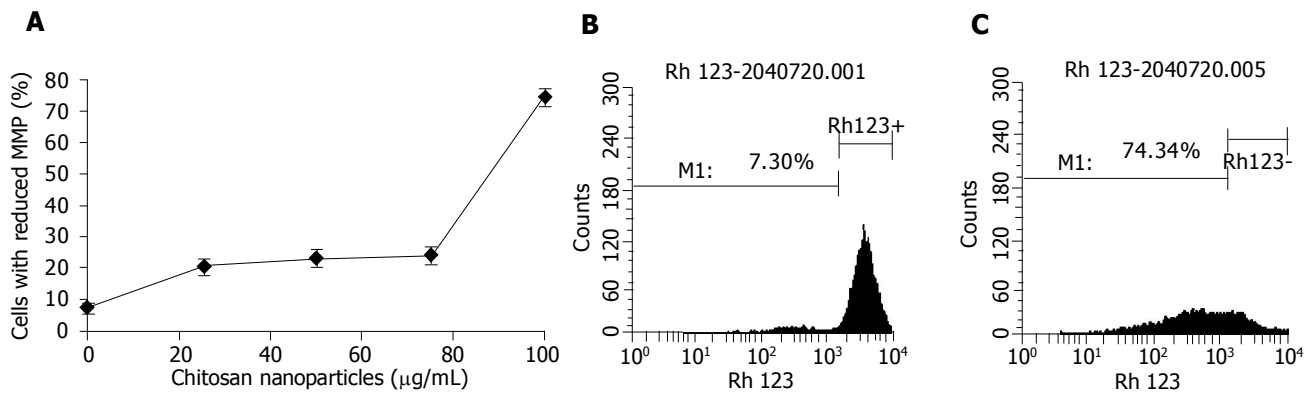


Figure 8 Chitosan nanoparticles-induced changes of MMP. **A:** Loss of MMP; **B:** histogram of untreated cells; **C:** histogram of cells treated with 100 µg/mL chitosan nanoparticles.

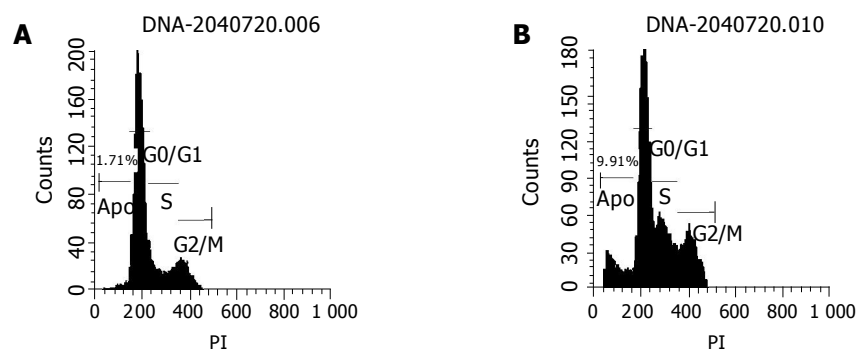


Figure 9 Effect of chitosan nanoparticles on cell cycle (A) and apoptotic incidence (B) of MGC803 cells.

Table 1 Effect of chitosan nanoparticles on cell cycle of MGC803 cells (mean±SD)

Concentration (µg/mL)	Cell cycle phase distribution (%)			AI
	G ₀ /G ₁	S	G ₂ /M	
0	71.8±1.3	17.3±0.9	9.5±0.2	1.7±0.2
25	70.5±0.8 ^b	16.7±1.1	8.3±2.1	3.9±0.6 ^b
50	69.4±0.6 ^b	15.9±0.6	7.4±0.3	6.8±0.3 ^b
75	67.3±0.4 ^b	13.2±2.3	12.3±0.5	7.6±0.4 ^b
100	51.5±1.3 ^b	23.5±1.1	15.2±3.1	9.9±0.5 ^b

AI: apoptotic incidence; ^bP<0.01 vs control.

of chitosan nanoparticles could be controlled only to 65 nm, which is in favor of the antitumor activity and prolongs efficacy of chitosan nanoparticles. Polymers with high cationic charge densities have higher cytotoxic effects than those with low charge densities^[24]. As a kind of cationic polymers, the surface charge of chitosan derivatives is the major factor affecting its cytotoxic activity due to the electrostatic ionic interaction between the negatively charged groups of tumor cells and the positively charged amino groups of chitosans^[19]. Therefore, the high surface charge about 52 mV of chitosan nanoparticles is responsible for its higher cytotoxic activity.

Morphologically, necrosis is quite different from apoptosis. During necrosis, cells first swell, then the plasma membrane collapses and cells are rapidly lysed, while apoptotic cells disintegrate into well-enclosed apoptotic bodies without loss of membrane integrity^[25]. The ultrastructural alterations of MGC803 cells observed by

electron microscopy displayed typical morphological features of necrosis due to the treatment of chitosan nanoparticles, suggesting that chitosan nanoparticles induce necrotic tumor cell death and can be used as a membrane-active drug. Chitosan nanoparticles are positively charged due to the cationic characteristics of chitosan^[26]. Chitosan nanoparticles could be first adsorbed onto the negatively charged tumor cell membrane by electrostatic interaction, then exhibit antitumoral effects by damaging membrane and disrupting organelle, and finally lead to cell death with the structure breakdown.

Fragmented DNA during apoptosis appears as a series of bands, which are described as “DNA ladders” on agarose gels, representing formation of oligonucleosomes with the characteristics of apoptosis^[27,28]. In contrast, fragmented DNA during necrosis appears as a continuous spectrum of sizes^[29]. In this study, chitosan nanoparticles-treated tumor

cells also yielded a continuous spectrum of DNA fragments of low molecular mass, indicating that necrosis is induced by chitosan nanoparticles.

It was reported that mitochondria play a crucial role in regulation of cell death^[30]. Under extreme conditions (e.g., high Ca²⁺, oxidative stress) mitochondria undergo drastic changes, accompanied with decrease of the mitochondrial potential, de-energization, swelling, and permeabilization of the inner membrane^[31]. Furthermore, the occurrence of mitochondrial dysfunction is rapidly followed by or nearly coincident with the loss of plasma membrane integrity^[32], thus leading to necrotic cell death at last. In this study, a drastic decrease of MMP was observed in chitosan nanoparticles-treated human gastric carcinoma cells, indicating that the mitochondrial membrane is damaged.

Cell cycle analysis showed a significant decrease of cells in the G₀/G₁ phase and the dose-dependent apoptosis in chitosan nanoparticles-treated cells, suggesting that apoptosis is also involved in the cell death induced by chitosan nanoparticles.

In summary, chitosan nanoparticles with a small particle size of about 65 nm and a positive surface charge of about 50 mV exhibit a high cytotoxicity towards human gastric carcinoma cell line MGC803 and induce cell death with predominant necrotic features. The antitumor mechanism of chitosan nanoparticles is related to their membrane-disrupting and apoptosis-inducing activities.

REFERENCES

- 1 **Qin C**, Du Y, Xiao L, Li Z, Gao X. Enzymic preparation of water-soluble chitosan and their antitumor activity. *Int J Biol Macromol* 2002; **31**: 111-117
- 2 **Roller S**, Covill N. The antifungal properties of chitosan in laboratory media and apple juice. *Int J Food Microbiol* 1999; **47**: 67-77
- 3 **Zheng LY**, Zhu JF. Study on antimicrobial activity of chitosan with different molecular weights. *Carbohydr Polym* 2003; **54**: 527-530
- 4 **Janes KA**, Fresneau MP, Marazuela A, Fabra A, Alonso MJ. Chitosan nanoparticles as delivery systems for doxorubicin. *J Control Release* 2001; **73**: 255-267
- 5 **Pan Y**, Li YJ, Zhao HY, Zheng JM, Xu H, Wei G, Hao JS, Cui FD. Bioadhesive polysaccharide in protein delivery system: chitosan nanoparticles improve the intestinal absorption of insulin *in vivo*. *Int J Pharm* 2002; **249**: 139-147
- 6 **Xu Y**, Du Y. Effect of molecular structure of chitosan on protein delivery properties of chitosan nanoparticles. *Int J Pharm* 2003; **250**: 215-226
- 7 **Qi L**, Xu Z, Jiang X, Hu C, Zou X. Preparation and antibacterial activity of chitosan nanoparticles. *Carbohydr Res* 2004; **339**: 2693-2700
- 8 **Qi LF**, Xu ZR. Lead sorption from aqueous solutions on chitosan nanoparticles. *Colloid Surface A* 2004; **251**: 183-190
- 9 **Qi L**, Xu Z, Jiang X, Li Y, Wang M. Cytotoxic activities of chitosan nanoparticles and copper-loaded nanoparticles. *Bioorg Med Chem Lett* 2005; **15**: 1397-1399
- 10 **Truter EJ**, Santos AS, Els WJ. Assessment of the antitumor activity of targeted immunospecific albumin microspheres loaded with cisplatin and 5-fluorouracil: toxicity against a rodent ovarian carcinoma *in vitro*. *Cell Biol Int* 2001; **25**: 51-59
- 11 **Luxo C**, Jurado AS, Madeira VM, Silva MT. Tamoxifen induces ultrastructural alterations in membranes of *Bacillus Stearothermophilus*. *Toxicol In Vitro* 2003; **17**: 623-628
- 12 **Kim H**, You S, Kong BW, Foster LK, Farris J, Foster DN. Necrotic cell death by hydrogen peroxide in immortal DF-1 chicken embryo fibroblast cells expressing deregulated MnSOD and catalase. *Biochim Biophys Acta* 2001; **1540**: 137-146
- 13 **Kok YJ**, Swe M, Sit KH. Necrosis has orderly DNA fragmentations. *Biochem Biophys Res Commun* 2002; **294**: 934-939
- 14 **Mi FL**, Tan YC, Liang HF, Sung HW. *In vivo* biocompatibility and degradability of a novel injectable-chitosan-based implant. *Biomaterials* 2002; **23**: 181-191
- 15 **Kim TH**, Park IK, Nah JW, Choi YJ, Cho CS. Galactosylated chitosan/DNA nanoparticles prepared using water-soluble chitosan as a gene carrier. *Biomaterials* 2004; **25**: 3783-3792
- 16 **Bivas-Benita M**, Laloup M, Verstehey S, Dewit J, Braekeleer JD, Jongert E, Borchard G. Generation of *Toxoplasma gondii* GRA1 protein and DNA vaccine loaded chitosan particles: preparation, characterization, and preliminary *in vivo* studies. *Int J Pharm* 2003; **266**: 17-27
- 17 **Mao HQ**, Roy K, Troung-Le VL, Janes KA, Lin KY, Wang Y, August JT, Leong KW. Chitosan-DNA nanoparticles as gene carriers: synthesis, characterization and transfection efficiency. *J Control Release* 2001; **70**: 399-421
- 18 **Carreno-Gomez B**, Duncan R. Evaluation of the biological properties of soluble chitosan and chitosan microspheres. *Int J Pharm* 1997; **148**: 231-240
- 19 **Lee JK**, Lim HS, Kim JH. Cytotoxic activity of aminoderivatized cationic chitosan derivatives. *Bioorg Med Chem Lett* 2002; **12**: 2949-2951
- 20 **Yokoyama M**, Satoh A, Sakurai Y, Okano T, Matsumura Y, Kakizoe T, Kataoka K. Incorporation of water-insoluble anticancer drug into polymeric micelles and control of their particle size. *J Control Release* 1998; **55**: 219-229
- 21 **Zhang L**, Hu Y, Jiang X, Yang C, Lu W, Yang YH. Camptothecin derivative-loaded poly(caprolactone-co-lactide)-b-PEG-b-poly (caprolactone-co-lactide) nanoparticles and their biodistribution in mice. *J Control Release* 2004; **96**: 135-148
- 22 **Jinno H**, Ikeda T, Matsui A, Kitagawa Y, Kitajima M, Fujii H, Nakamura K, Kubo A. Sentinel lymph node biopsy in breast cancer using technetium-99m tin colloids of different sizes. *Biomed Pharmacother* 2002; **56** (Suppl 1): 213s-216s
- 23 **Takenaga M**. Application of lipid microspheres for the treatment of cancer. *Adv Drug Deliv Rev* 1996; **20**: 209-219
- 24 **Fischer D**, Li Y, Ahlemeyer B, Kriegelstein J, Kissel T. In vitro cytotoxicity testing of polycations: influence of polymer structure on cell viability and hemolysis. *Biomaterials* 2003; **24**: 1121-1131
- 25 **Proskuryakov SY**, Konoplyannikov AG, Gabai VL. Necrosis: a specific form of programmed cell death? *Exp Cell Res* 2003; **283**: 1-16
- 26 **Hu Y**, Jiang X, Ding Y, Ge H, Yuan Y, Yang C. Synthesis and characterization of chitosan-poly(acrylic acid) nanoparticles. *Biomaterials* 2002; **23**: 3193-3201
- 27 **Zhao Y**, Cao J, Ma H, Liu J. Apoptosis induced by tea polyphenols in HL-60 cells. *Cancer Lett* 1997; **121**: 163-167
- 28 **Kono T**, Watanabe M, Koyama K, Kishimoto T, Fukushima S, Sugimura T, Wakabayashi K. Cytotoxic activity of pierisin, from the cabbage butterfly, *Pieris rapae*, in various human cancer cell lines. *Cancer Lett* 1999; **137**: 75-81
- 29 **Bicknell GR**, Cohen GM. Cleavage of DNA to large kilobase pair fragments occurs in some forms of necrosis as well as apoptosis. *Biochem Biophys Res Commun* 1995; **207**: 40-47
- 30 **Monti MG**, Ghiaroni S, Marverti G, Montanari M, Moruzzi MS. Polyamine depletion switches the form of 2-deoxy-d-riboseinduced cell death from apoptosis to necrosis in HL-60 cells. *Int J Biochem Cell B* 2004; **36**: 1238-1248
- 31 **Lemasters JJ**, Qian T, Bradham CA, Brenner DA, Cascio WE, Trost LC, Nishimura Y, Nieminen AL, Herman B. Mitochondrial dysfunction in the pathogenesis of necrotic and apoptotic cell death. *J Bioenerg Biomembr* 1999; **31**: 305-319
- 32 **Bonneau MJ**, Poulin R. Spermine oxidation leads to necrosis with plasma membrane phosphatidylserine redistribution in mouse leukemia cells. *Exp Cell Res* 2000; **259**: 23-34